Dispersion of Transient Signals in Microstrip Transmission Lines

RICHARD L. VEGHTE, MEMBER, IEEE, AND CONSTANTINE A. BALANIS, FELLOW, IEEE

Abstract — **The distortion of an electrical pulse caused by dispersion as it propagates along a microstrip line is investigated. A model for dispersion of the phase constant is selected to meet the frequency, accuracy, and microstrip parametric requirements. Numerical integration and Taylor series expansion approximation techniques are used to compute the shape of dc dispersed pulses having square and Gaussian envelope shapes. Taylor series expansion methods are more convenient for the analysis of RF pulses.**

I. Introduction

THE DESIGN of MIC's requires a knowledge of switching and transient signal behavior in microstrip transmission lines and semiconductor structures. The distortion of dc and RF pulses in waveguides and dispersive materials has received, in the past, considerable attention [1]–[3]. However, distortion of pulses, both dc and RF, in microstrip lines has not yet been examined thoroughly [4].

As an electrical pulse travels along a microstrip line, it becomes distorted due to the dispersion and attenuation characteristics of the line. While the electric and magnetic fields are confined to one material in waveguides, coaxial lines and striplines, the microstrip is open so that the fields are partially in the air and partially in the dielectric. The air–dielectric interface prevents propagation of a pure TEM mode. Therefore, the phase constant is not a linear function of frequency, and it results in dispersion.

Below a certain frequency (f_t), the propagation is approximately TEM and dispersion is virtually nonexistent. Pulses which have a spectral content above f_t will be dispersed since the higher harmonics of the pulse will travel at a slower velocity than the lower harmonics. This paper combines existing microstrip dispersion formulas and analytical techniques to examine in microstrips the dispersed shape of dc and RF pulses having square and Gaussian envelope shapes.

II. Distortion of Signals

The voltage or electric field at $z = 0$ (a reference point in the microstrip line) is represented by

$$v(t, z=0) = \begin{cases} v(t), & -T/2 \leqslant t \leqslant T/2 \\ 0, & \text{elsewhere} \end{cases}. \tag{1}$$

Manuscript received March 15, 1986; revised June 6, 1986. This work was supported in part by the U.S. Army Research Office under Research Contract DAAG29-85-K-0078.

R. L. Veghte was with the Department of Electrical and Computer Engineering, Arizona State University, Tempe. He is now with Ball Aerospace Systems Division, Boulder, CO 80306.

C. A. Balanis is with the Department of Electrical and Computer Engineering, Arizona State University, Tempe, AZ 85287.

IEEE Log Number 8610564.

In the frequency domain, the signal can be written as

$$V(\omega, z=0) = \int_{-T/2}^{T/2} v(t, z=0) e^{-j\omega t}\, dt \tag{2}$$

where $V(\omega)$ and $v(t)$ form a transform pair. For certain transient signals, such as a square pulse, the limits $-T/2 \leqslant t \leqslant T/2$ define the pulsewidth, and the signal is confined to a short time period. For a Gaussian pulse, the time range of $-\infty < t < \infty$ is needed to completely characterize the response.

At a distance L, the signal (or pulse) in the frequency domain becomes

$$V(\omega, z=L) = V(\omega, z=0) e^{-\gamma(\omega)L}. \tag{3}$$

The frequency-dependent propagation constant is

$$\gamma(\omega) = \alpha(\omega) + j\beta(\omega) \tag{3a}$$

where $\alpha(\omega)$ and $\beta(\omega)$ are, respectively, the attenuation and phase constants. For this investigation, the frequency-dependent attenuation constant $\alpha(\omega)$ is assumed to be negligible, so that (3) reduces to

$$V(\omega, z=L) = V(\omega, z=0) e^{-j\beta(\omega)L}. \tag{4}$$

Taking the inverse transform of (4) leads to the time-domain representation of the pulse at $z = L$, and it can be written as

$$\begin{aligned} v(t, L) &= \frac{1}{2\pi} \int_{-\infty}^{\infty} V(\omega, z=L) e^{+j\omega t}\, d\omega \\ &= \frac{1}{2\pi} \int_{-\infty}^{\infty} V(\omega, z=0) e^{j[\omega t - \beta(\omega)L]}\, d\omega. \end{aligned} \tag{5}$$

For lossless lines, the phase constant $\beta(\omega)$ can be written as

$$\beta(\omega) = \omega\sqrt{\mu\epsilon(\omega)} = \frac{\omega}{c}\sqrt{\epsilon_{r_{\text{eff}}}(\omega)}. \tag{6}$$

The expression $V(\omega, z = 0)$, the transform of $v(t,0)$, is easily obtained for many common waveshapes such as square, Gaussian, triangular dc pulses, and any RF wave modulated by these pulses. The transforms of more complex waveforms can be constructed using these basic waveforms.

The Fourier transform of a Gaussian pulse whose time-domain representation is

$$f(t) = A \exp(-a^2 t^2) \tag{7}$$

is given by [5]

$$F(\omega) = \frac{A\sqrt{\pi}}{a} \exp(-\omega^2/4a^2) \tag{8}$$

0018-9480/86/1200-1427$01.00 ©1986 IEEE

where $2/a$ is the 3-dB pulsewidth and A is the amplitude of the pulse in the time domain. For a square pulse, the time-domain representation is

$$f(t) = \begin{cases} A, & -L \leqslant t \leqslant L \\ 0, & \text{otherwise} \end{cases} \tag{9}$$

while its Fourier transform is [5]

$$F(\omega) = 2A \frac{\sin(L\omega)}{\omega} \tag{10}$$

where $2L$ is the pulsewidth and A is the amplitude of the pulse.

The Fourier transform of an RF pulse with a carrier frequency ω_0 has the same form as the dc pulse, but it is split into two equal components, one of which is shifted up in frequency and the other is shifted down. For example, a square pulse with a time-domain representation of

$$f(t) = \begin{cases} A\cos\omega_0 t, & -L \leqslant t \leqslant L \\ 0, & \text{otherwise} \end{cases} \tag{11}$$

has a Fourier transform of

$$F(\omega) = A\left[\frac{\sin[L(\omega-\omega_0)]}{(\omega-\omega_0)} + \frac{\sin[L(\omega+\omega_0)]}{(\omega+\omega_0)}\right]. \tag{12}$$

Fourier transforms, instead of Laplace transforms, are used to analyze the pulses because they are more convenient for the interpretation of the dispersion characteristics from the real frequency spectrum point of view. This is very attractive for the examination of the effective dielectric constant variations as a function of frequency and their impact upon the dispersion of the pulses.

III. Frequency-Dependent Phase Constant

Numerous methods have been used to determine $\epsilon_{r_{\text{eff}}}(\omega)$ for microstrip lines. Many papers use full-wave solutions such as the spectral-domain [6] or transverse current distribution methods [7]. These full-wave solutions have been examined [8], compared to other methods, and been found to be quite accurate. However, these methods depend on time-consuming computations and not on closed-form equations, which would be most desirable when confronted with the evaluation of (5). Some papers have curve-fitted equations for $\epsilon_{r_{\text{eff}}}(\omega)$ which are simple to use. However, none of these equations extend above 20 GHz, and they are not adequate for many transient signals that have frequency components up to 100–200 GHz.

Two methods that may be used to calculate $\epsilon_{r_{\text{eff}}}(\omega)$ which provide physical insight and fairly simple closed-form expressions, although they may not be as accurate as the full-wave analysis, are 1) coupled modes (TEM, TE, and TM modes) [9], [10] and 2) single longitudinal section electric (LSE) [11].

Equations which use coupled modes are given by Schneider [12] (TEM/TE), Carlin [13] (TE/TM), Kobayashi [14] (TEM/TM), Pramanick and Bhartia [15] (TEM/TE), and Yamashita [16] (curve fitting using the TE mode). Getsinger [11] uses the LSE model to determine the frequency-dependent dielectric constant, while Kirching and Jansen [17] curve-fit results from a full-wave, spectral-domain analysis. From the standpoint of analytical rigor, simplicity, and agreement with other existing data, it was found that the model for $\epsilon_{r_{\text{eff}}}(\omega)$ of Pramanick and Bhartia [15] was as accurate as any of the others. For this model $\epsilon_{r_{\text{eff}}}(\omega)$ is expressed as

$$\epsilon_{r_{\text{eff}}}(f) = \epsilon_r - \frac{\epsilon_r - \epsilon_{r_{\text{eff}}}(0)}{1 + \dfrac{\epsilon_{r_{\text{eff}}}(0)}{\epsilon_r}\left(\dfrac{f}{f_t}\right)^2} \tag{13}$$

where

$$f_t = \frac{Z_0}{2\mu_0 h} \tag{13a}$$

ϵ_r relative dielectric constant of the substrate,
$\epsilon_{r_{\text{eff}}}(0)$ effective relative dielectric constant at zero frequency,
h height of microstrip line above ground plane,
Z_0 characteristic impedance of microstrip line,
μ_0 free-space permeability.

IV. Evaluation of Integral Equation

Three different methods to evaluate the integral of (5) are examined in this section. The complexity of the frequency-dependent phase constant $\beta(\omega)$ precludes solving for the integral in closed form. Thus, numerical integration techniques are examined, and a quadratic approximation to $\beta(\omega)$ (the Taylor series expansion method) is used to evaluate the integral of (5). The method of stationary phase is also examined as a possible technique to evaluate (5).

Numerical integration is the most straightforward technique for evaluating (5), but its accuracy depends on the amount of computer time and storage space available. DC pulses use less computer resources than RF pulses and this method is best suited for them. The Taylor series expansion method [1] is an approximation to the full integration of (5). It is slightly less accurate than numerical integration, but it requires much less computer time to evaluate the integral, especially for RF pulses.

In (5), the limits of integration are $-\infty < \omega < \infty$; however, beyond a certain radian frequency ω_L, the contributions to the integral are negligible. Narrower pulses have a higher frequency content and thus will need a higher ω_L; thus, significant parts of the integral are not excluded. If τ is the width of the pulse, then

$$\omega_L = \zeta/\tau \tag{14}$$

where ζ is a constant which depends on the waveshape. For example, for a square pulse with a sharp rise time (high frequency content), ζ is about 500. For a Gaussian pulse with a slower rise time, a ζ of 20 is sufficient. Thus, (5) becomes

$$v(t, L) \cong \frac{1}{2\pi}\int_{-\zeta/\tau}^{\zeta/\tau} V(\omega, z=0)\, e^{j[\omega t - \beta(\omega)L]}\, d\omega. \tag{15}$$

This can be written as a series approximation of the form

$$v(t, L) \cong \frac{1}{2\pi} \sum_{i=1}^{N} V(\omega_i, z=0) e^{j[\omega_i t - \beta(\omega_i) L]} \Delta\omega_i \quad (16)$$

where N is the number of divisions in the frequency spectrum and $\Delta\omega (= 2\zeta/\tau/N)$ is the width of each uniform segment. Since we are concerned only with the real part of the pulse, (16) becomes

$$v(t, L) \cong \frac{1}{2\pi} \sum_{i=1}^{N} V(\omega_i, z=0) \cos\left[\omega_i t - \beta(\omega_i) L\right] \Delta\omega_i. \quad (17)$$

Equation (17) is easily programmed on the computer once $V(\omega_i, z=0)$, the Fourier transform of the pulse being considered, is known.

In addition to using numerical integration to evaluate (5), there are approximate methods which can represent it in closed form. One such method is the Taylor series expansion, where the phase constant $\beta(\omega)$ is represented by a Taylor series of [1], [2]

$$\beta(\omega) = \beta(\omega_0) + \beta'(\omega_0)(\omega - \omega_0) + \frac{1}{2}\beta''(\omega_0)(\omega - \omega_0)^2 \cdots. \quad (18)$$

The first three terms of the Taylor series expansion are used to approximate the phase constant in the vicinity of ω_0. This is referred to as the *quadratic approximation*. For the cases being investigated, it is a good assumption to consider the phase constant to be a quadratic function of frequency. If the pulses are sufficiently wide compared to the carrier frequency, then only a small segment of the $\beta(\omega)$ curve is used and such an approximation is valid. The expressions for $\beta'(\omega_0)$ and $\beta''(\omega_0)$ are

$$\beta'(\omega_0) = \left.\frac{\partial\beta}{\partial\omega}\right|_{\omega=\omega_0} \quad (19)$$

$$\beta''(\omega_0) = \left.\frac{\partial^2\beta}{\partial\omega^2}\right|_{\omega=\omega_0} \quad (20)$$

It is possible to obtain closed-form solutions to (5) using the quadratic approximation if the signal in the frequency domain at $z=0$, $V(\omega, z=0)$, can be written in closed form. Closed-form expressions have been derived to evaluate (5) for Gaussian [1] and square [2], [3] RF-modulated pulses dispersed as they travel in a waveguide. These equations were modified for microstrips, where the frequency-dependent $\beta(\omega)$ of (6) was formed using Pramanick and Bhartia's model [15] for $\epsilon_{r_{\text{eff}}}(\omega)$.

The method of stationary phase [18] is used to evaluate integrals of the form

$$I(t) = \int_{-\infty}^{\infty} F(\omega) e^{jt\mu(\omega)} d\omega \overset{t\to\text{large}}{\simeq} \sqrt{\frac{2\pi}{-t\mu''(\omega_s)}}\, F(\omega_s) e^{t\mu(\omega_s)} \quad (21)$$

where ω_s represents the stationary phase point obtained using

$$\mu'(\omega_s) = 1 - \frac{L}{t}\beta'(\omega_s) = 0. \quad (21a)$$

Equation (5) can be rearranged so that it is of the form

$$V(t, L) = \frac{1}{2\pi}\int_{-\infty}^{\infty} V(\omega, z=0) e^{jt[\omega - \beta(\omega)L/t]} d\omega. \quad (22)$$

Comparing (21) and (22), it is apparent that

$$F(\omega) = \frac{1}{2\pi} V(\omega, z=0) \quad (22a)$$

and

$$\mu(\omega) = \omega - \beta(\omega)\frac{L}{t}. \quad (22b)$$

It was found that for a given distance L that the pulse had traveled, the stationary phase point could only be found for certain "windows" of time. The windows of time for the cases investigated were found to correspond to the location of the pulses; however, the time interval was too short to include the entire pulse in most cases. Therefore, this technique was found to have limited utility.

V. Computations

The investigation of possible dispersion models for microstrip transmission lines revealed that there are numerous candidates to choose from. The selection process became even more difficult given the fact that there is no conclusive experimental data for a frequency-dependent phase constant for microstrip at higher frequencies (above 20 GHz). Thus, it was necessary to compare the existing methods with each other in order to identify an acceptable accurate method. When investigating the frequency-dependent phase constant $\beta(\omega)$, it was found that most papers and books dealt with the frequency-dependent effective relative dielectric constant $\epsilon_{r_{\text{eff}}}(\omega)$; the two constants are related by (6).

The six most promising dispersion equations are those of Getsinger [11], Pramanick and Bhartia [15], Yamashita [16], Carlin [13], Schneider [12], and Kobayashi [14]. These were initially chosen because they were valid for high frequencies (up to 100–200 GHz), which will allow the analysis of short pulses and pulses with high frequency content (sharp rise times). These six models cover a wide range of dielectric constants and microstrip geometries. Also, these models can be related to the physical microstrip line so that conclusions about the dispersed pulse can be traced to properties of the microstrip line.

A frequency range of 1 to 10 000 GHz was used to cover the entire dispersive region of possible microstrip transmission lines. The results for various dielectric constants and different widths and heights of the microstrip line were investigated. Dielectric constants of 2.33, 3.78, 6.80, 10.2, and 13.0 were chosen to represent, respectively, duroid-type materials, fused silica, beryllium oxide, alumina (or similar soft substrates), and gallium arsenide. Microstrip line heights were selected to represent the commonly available

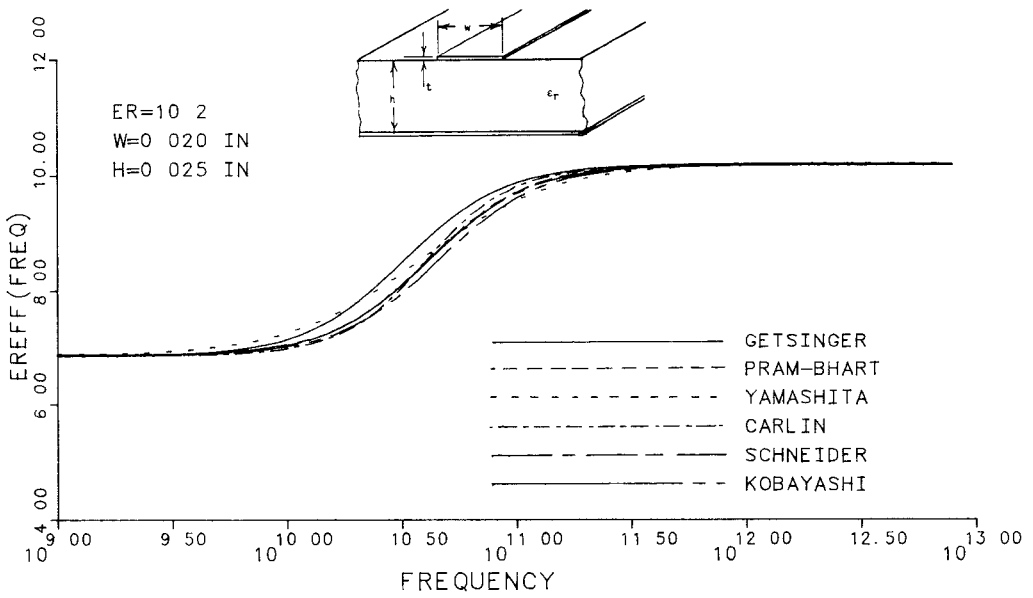

Fig. 1. Effective dielectric constant of a microstrip line as a function of frequency for different proposed models ($\epsilon_r = 10.2$, $w/h < 1.0$).

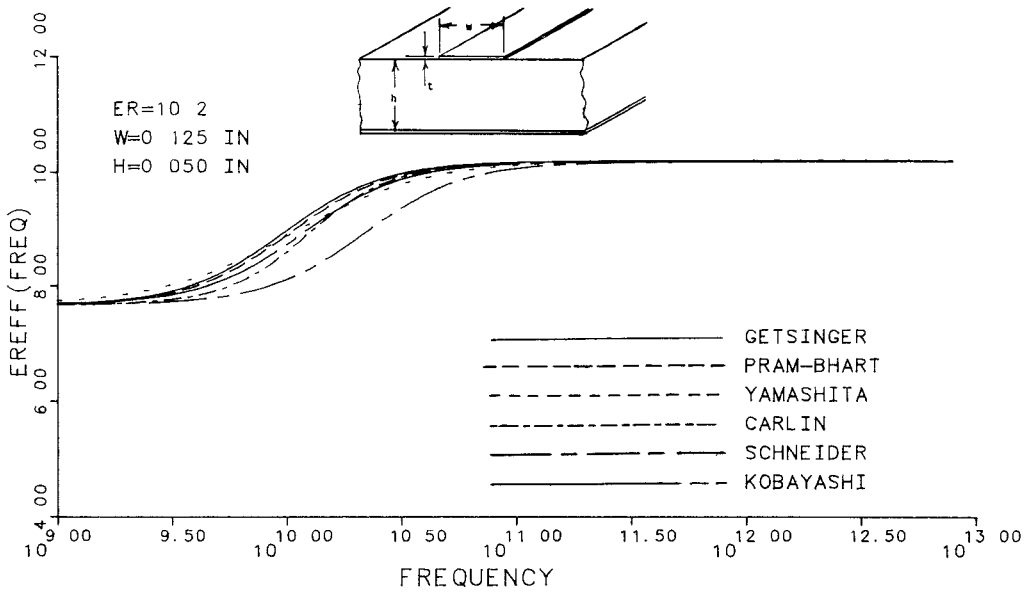

Fig. 2. Effective dielectric constant of a microstrip line as a function of frequency for different proposed models ($\epsilon_r = 10.2$, $w/h > 1.0$).

substrate thickness of the various materials. The line widths were determined so that the w/h ratio was less than and greater than unity. The widths also were chosen so that the impedances of the lines were on the order of 10–100 Ω and were realizable using current fabrication techniques.

The variations of $\epsilon_{r_{\text{eff}}}(\omega)$ as a function of frequency for six different models are shown in Figs 1 and 2. Those in Fig. 1 are representative for a microstrip with $\epsilon_r = 10.2$, $w = 0.020$ in, $h = 0.025$ in ($w/h = 0.8 < 1$), while those in Fig. 2 are for a microstrip with $\epsilon_r = 10.2$, $w = 0.125$ in, $h = 0.050$ in ($w/h = 2.5 > 1$). The data in these figures illustrate how the relative effective dielectric constant starts at $\epsilon_{r_{\text{eff}}}(0)$ for low frequencies and then increases to ϵ_r, the dielectric constant of the material, at high frequencies.

Before proceeding with the comparison of different dispersed pulses that use the different models for $\epsilon_{r_{\text{eff}}}(\omega)$, it will be convenient to eliminate two of the models. Carlin's dispersion formula was eliminated since it has the same characteristics as some of the other models. Schneider's dispersion model was in close agreement with the other models for narrow lines, but it was consistently shifted toward higher frequencies for the wider lines (as in Fig. 2). Kobayashi has included a factor which corrects this problem.

The distortion of a $\tau = 10$ ps (3-dB width) dc Gaussian pulse, as predicted using four of these models, traveling a distance $L = 0.354$ in along a microstrip whose parameters and dimensions are the same as those in Fig. 1 is displayed

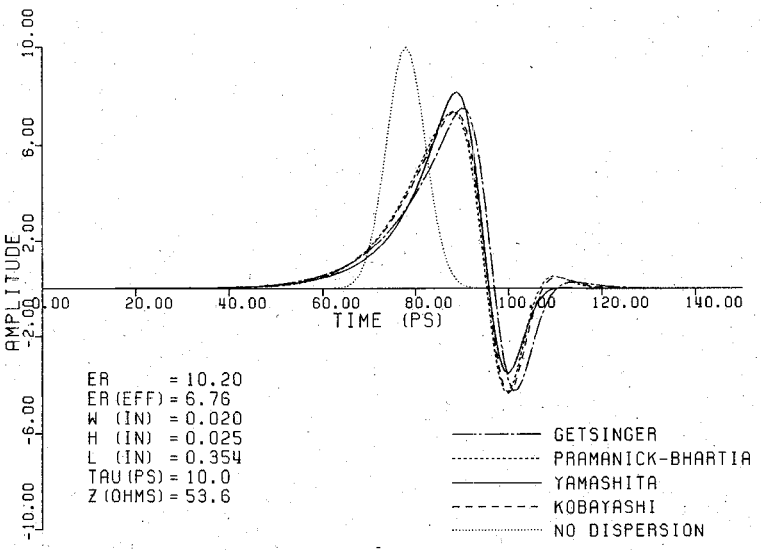

Fig. 3. Gaussian dc pulse dispersion at a distance $L = 0.354$ in (0.90 cm) in a microstrip line using different proposed models for the effective dielectric constant ($\epsilon_r = 10.2$, $w/h < 1.0$).

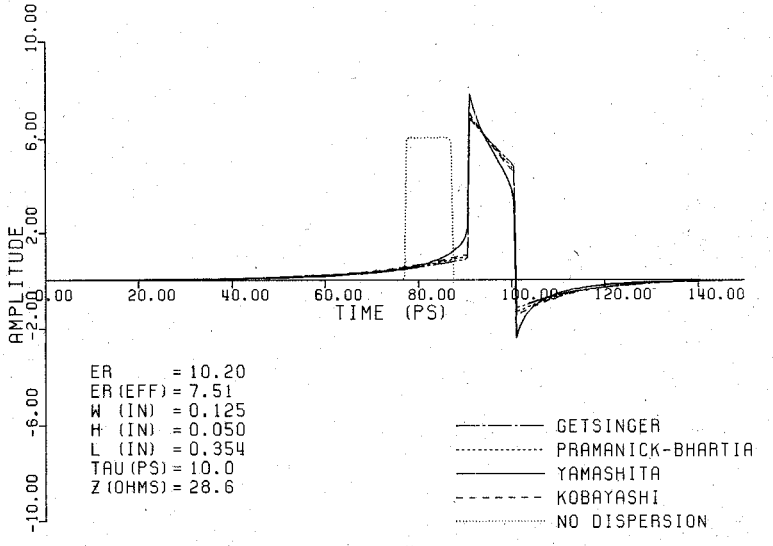

Fig. 4. Square dc pulse dispersion at a distance $L = 0.354$ in (0.90 cm) in a microstrip line using different proposed models for the effective dielectric constant ($\epsilon_r = 10.2$, $w/h > 1.0$).

in Fig. 3. For comparison, the undistorted pulse is also exhibited in the figure. The position of the undistorted pulse has been determined assuming that its velocity of propagation is based on the effective dielectric constant of the microstrip at zero frequency. The waveforms of the distorted pulses were computed using numerical integration for the evaluation of (5), as outlined in Section IV. The distorted waveforms of a dc square pulse of 10 ps obtained using numerical integration and traveling a distance $L = 0.354$ in along a microstrip line whose parameters and dimensions are the same as those in Fig. 2 are shown in Fig. 4. The undistorted pulse is also displayed for comparison. It is observed, especially in the undistorted square pulse, that very small localized spikes appear at its leading and trailing edges. These spikes are spurious and are a consequence of Gibbs's phenomenon associated with Fourier transforms. Proper choice of the sampling points can reduce their impact.

The comparison of the dispersion models in Figs. 3 and 4 reveals that the small differences in $\epsilon_{r_{\text{eff}}}(\omega)$ translate into small differences in the dispersed waveform. The differences in the dispersed pulse (different amplitude, pulsewidth, and ringing) are particularly small for pulses with a narrow spectrum, such as the Gaussian pulse. The dispersed waveforms are still quite similar for pulses with a wide spectral content, such as the square pulse.

Considering the similarities between the dispersed pulses using the dispersion models of Getsinger, Pramanick and Bhartia, Yamashita, and Kobayashi, any of these four dispersion equations would be acceptable for determining the shape of a pulse as it travels along a microstrip line. However, Pramanick and Bhartia's, and Getsinger's dis-

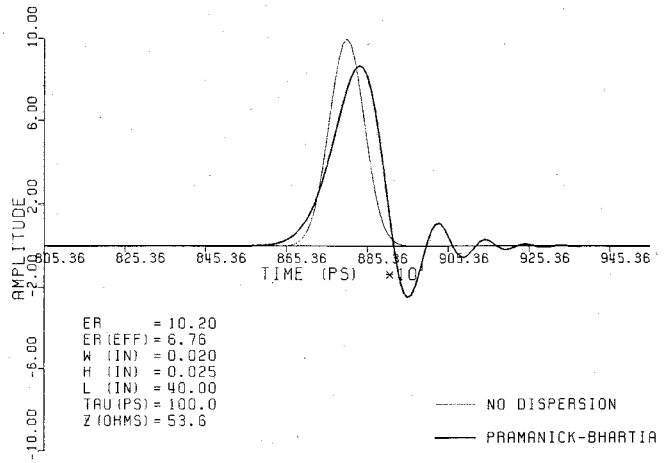

Fig. 5. Gaussian dc pulse dispersion at a distance $L = 40$ in (101.6 cm) along a microstrip line ($\epsilon_r = 10.2$, $w/h < 1.0$).

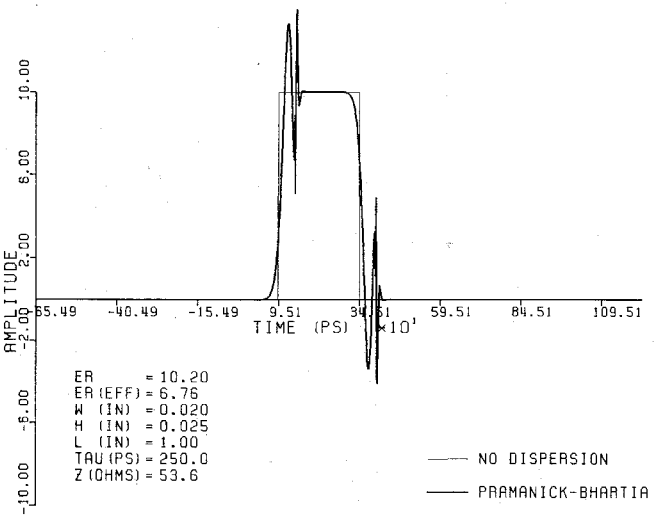

Fig. 6. Square dc pulse dispersion at a distance $L = 1$ in (2.54 cm) along a microstrip line ($\epsilon_r = 10.2$, $w/h < 1.0$).

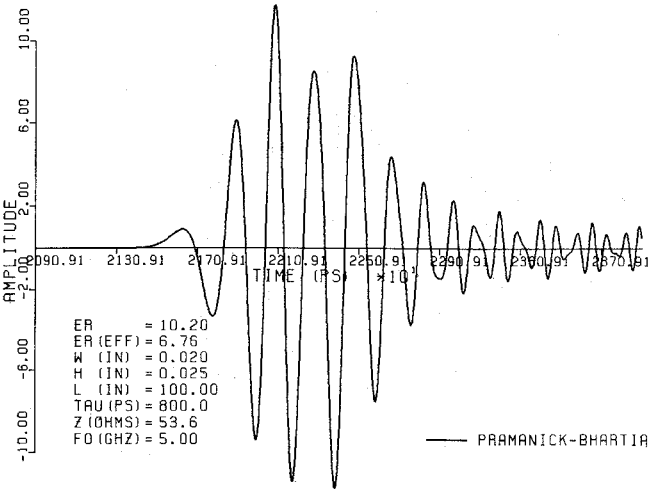

Fig. 7. Square RF pulse with a carrier frequency of 5 GHz at a distance $L = 100$ in (254 cm) along a microstrip line ($\epsilon_r = 10.2$, $w/h < 1.0$).

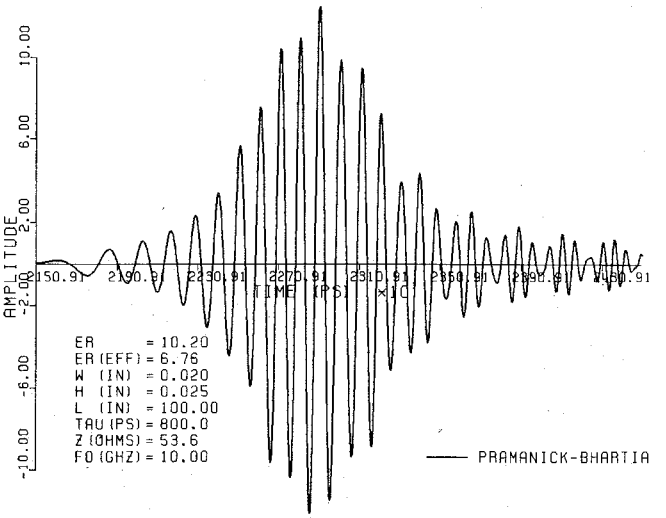

Fig. 8. Square RF pulse with a carrier frequency of 10 GHz at a distance $L = 100$ in (254 cm) along a microstrip line ($\epsilon_r = 10.2$, $w/h < 1.0$).

persion formulas look more promising due to their simpler formulation. If numerical integration is used, the simpler final expressions for $\epsilon_{r_{\text{eff}}}(\omega)$ are significant since they will be evaluated thousands of times for each pulse. If the Taylor series expansion method is used, it will be easier to take the first and second derivatives of the phase constant if either of these two models is used.

In order to choose between Getsinger's model and Pramanick and Bhartia's equation, the question of accuracy arises. Since both equations are in the same form, the choice of the inflection frequency is the only difference between the two. Getsinger's inflection frequency is always lower than the one given by Pramanick and Bhartia. Getsinger uses the LSE analysis to determine the inflection frequency, while Pramanick and Bhartia use an inflection frequency related to the cutoff frequency of the TE_1 mode which is derived from coupled-mode theory. The inflection frequency from the coupled-mode theory will be more accurate than that derived using a LSE analysis. This is confirmed by the fact that the other four dispersion formulas all had inflection frequencies that were close to Pramanick and Bhartia's while Getsinger's formulas always produced an inflection frequency that was lower than all of the others. So, although Getsinger's equations were the first ones (and the ones that the others are often compared to) and while the other four equations would be satisfactory, Pramanick and Bhartia's model for $\epsilon_{r_{\text{eff}}}$ [15] was chosen for the continuation of the investigation of pulse distortion due to dispersion.

The distortion of a $\tau = 100$ ps (3-dB width) dc Gaussian pulse that has traveled 40 in along a microstrip line with $\epsilon_r = 10.2$, width = 0.020 in and height = 0.025 in is displaced in Fig. 5. The peak amplitude has attenuated, the pulse is wider, and ringing is evident. This is typical of a Gaussian dc pulse with low spectral content. A square dc pulse that has a width of 250 ps and has traveled 1 in

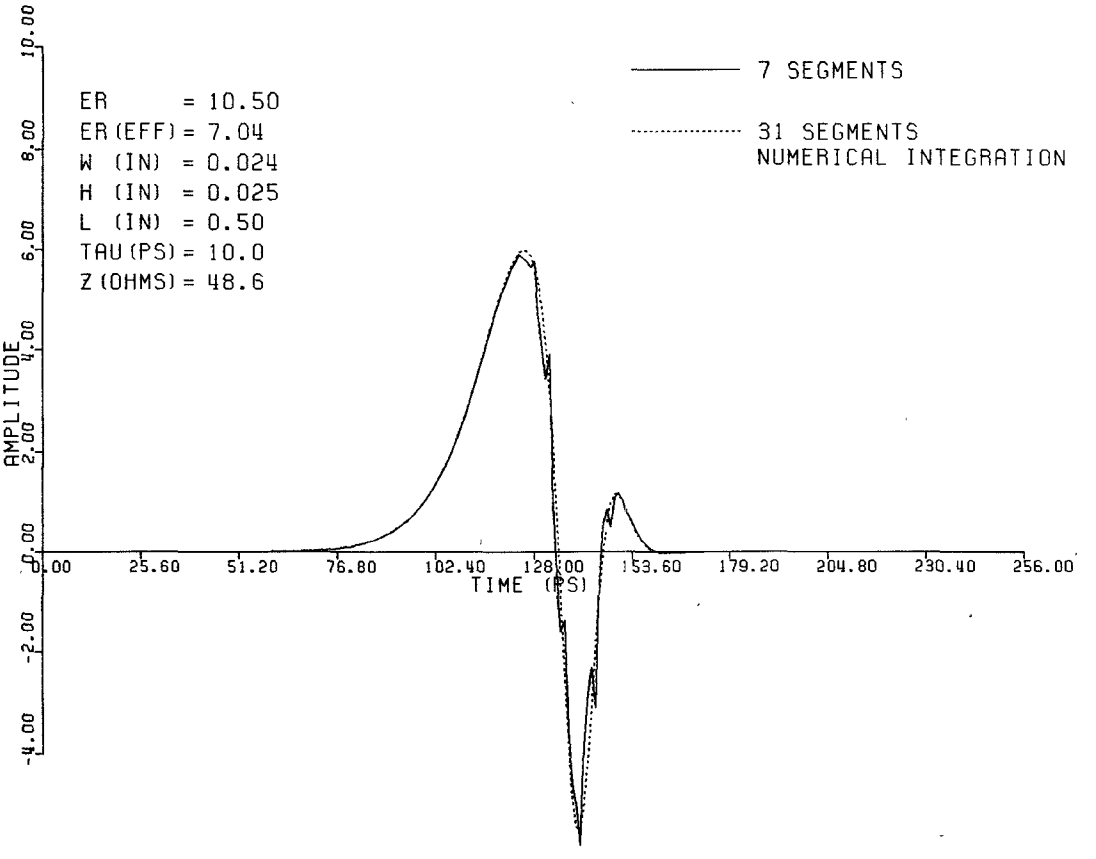

Fig. 9. Dispersed dc Gaussian pulse computed using seven and 31 segments, each of 4 ps, and numerical integration.

along a microstrip line with $\epsilon_r = 10.2$, $w = 0.025$ in, and $h = 0.025$ in is shown in Fig. 6. It is apparent that major distortion peaks along the leading and trailing edges have been created by the separation of the high and low spectral components of the square pulse. This is typical of square dc pulses, which have a much higher spectral content than the comparable Gaussian pulse.

The pulses in Figs. 7 and 8 are square RF pulses which have traveled 100 in along a microstrip line with $\epsilon_r = 10.2$, $w = 0.020$ in, and $h = 0.025$ in. The square RF pulse in Fig. 7 has a lower carrier frequency (5 GHz) which is located in a region of the $\epsilon_{r_{\text{eff}}}(\omega)$ versus frequency curve (Fig. 1) where little dispersion is occurring. Fig. 8 is the same pulse, but with a carrier frequency of 10 GHz. It is much more dispersed, since the carrier frequency is located in a region of Fig. 1 where more dispersion is occurring. Figs. 5 through 8 were computed using numerical integration and Pramanick and Bhartia's dispersion formula.

For some microstrip dispersion problems, a square, Gaussian, or triangular pulse may not be a good approximation to the shape of the actual pulse being investigated. For these and other cases, where closed-form solutions may not be available for the Fourier transform, it will be necessary to segment the pulse into a number of square pulses and then to add the contributions from each of the subsegments. After dispersing the individual subsegmented square pulses, the results are added together to get the entire dispersed arbitrary pulse.

To test this method, a pulse shape which is already known (a Gaussian pulse) was subdivided into rectangular segments. The dispersed waveform was then computed by using the partitioning method. A dispersed Gaussian pulse which was obtained using seven rectangular segments is shown in Fig. 9. When this dispersed, segmented pulse is compared in Fig. 9 to a dispersed Gaussian pulse which is obtained by using the numerical integration method, it is noted that some differences appear. The pulse that was re-created using seven segments is not as smooth as it should be; this is caused by the coarse partitioning that was used. If, however, the pulse was divided into 31 square segments before it was dispersed, the dispersed pulse does not differ from the Gaussian pulse computed using the normal numerical method, as shown in Fig. 9. This partitioning process can be used to analyze the distortion of any shape pulse, such as a stepped pulse, shown in Fig. 10. Horizontal segmentation can be applied with similar success.

To compare the validity of the Taylor series approximation method of Section IV, computations were made for the envelope of distorted Gaussian and square RF pulses using the Taylor series expansion method. The envelopes of the distorted pulses were obtained using Forrer's [1] formulations for Gaussian pulses and Knop's [3] equations for square pulses.

Using Pramanick and Bhartia's model for $\epsilon_{r_{\text{eff}}}(\omega)$, the frequency-dependent phase constant and its first and sec-

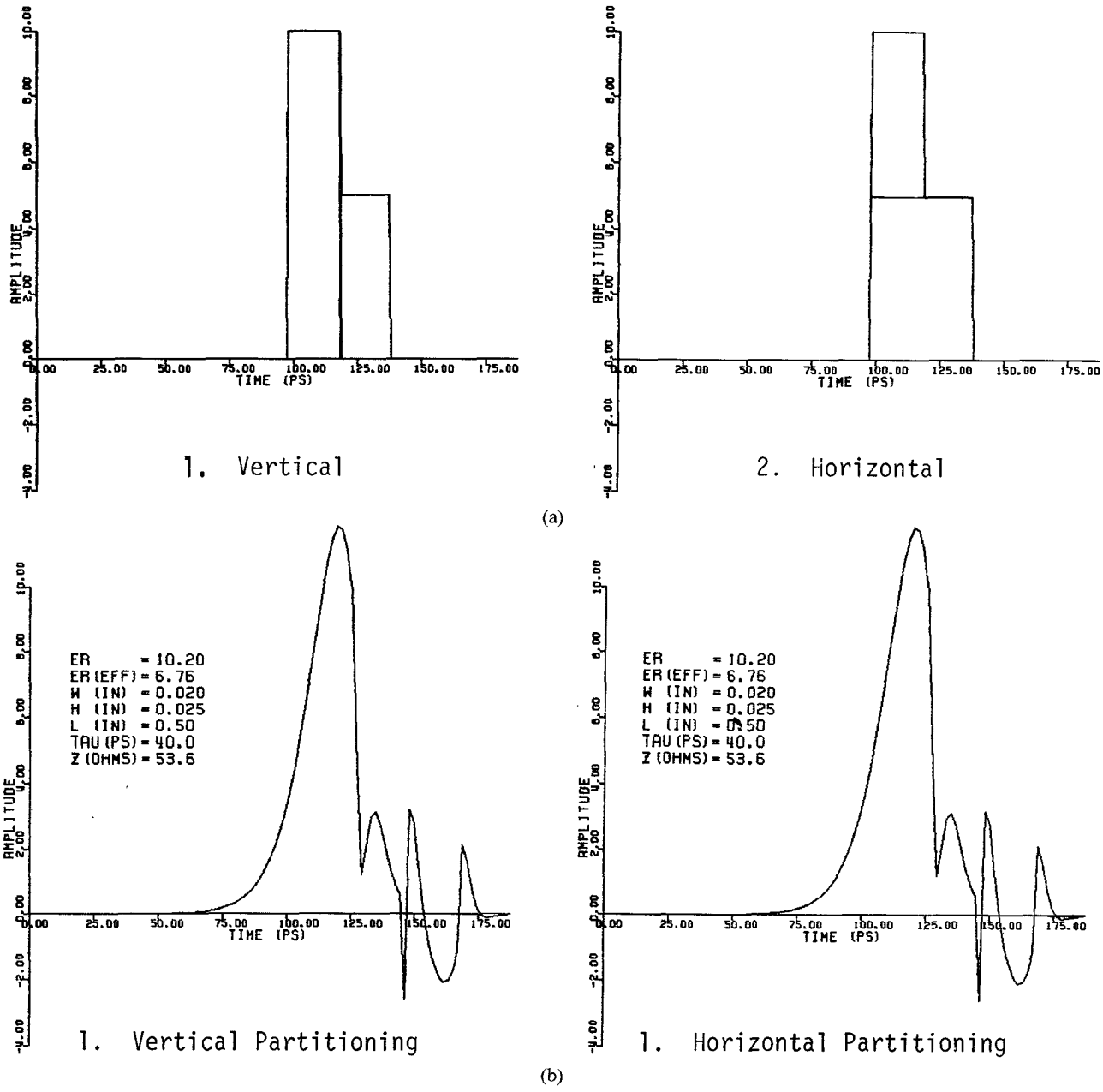

Fig. 10. (a) Pulse partitioning and (b) dispersed dc stepped rectangular pulse using segmented method of vertical and horizontal segments.

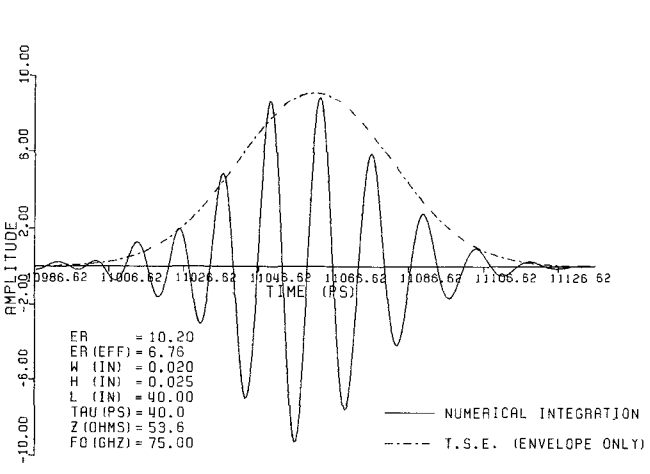

Fig. 11. Comparison of numerical integration and Taylor series expansion method for an RF Gaussian pulse (carrier frequency = 75 GHz).

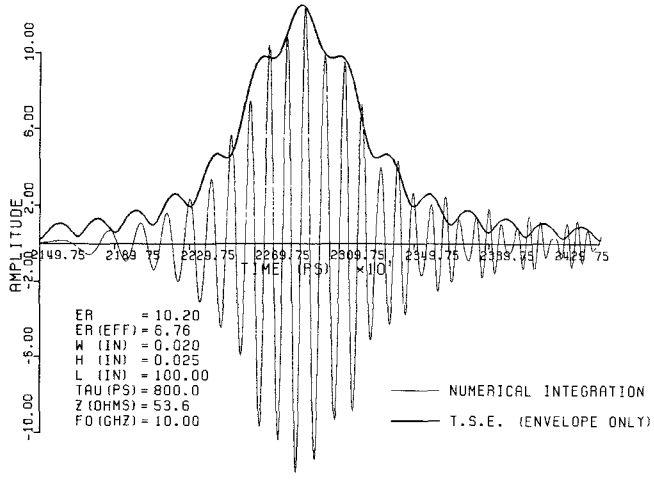

Fig. 12. Comparison of numerical integration and Taylor series expansion method for an RF square pulse (carrier frequency = 10.0 GHz).

TABLE I
APPROXIMATE CPU TIME FOR TYPICAL DISPERSED PULSES USING VARIOUS METHOD OF ANALYSIS

	Numerical Techniques	Taylor Series Expansion Method	Method of Stationary Phase
DC Gaussian Pulse	15 sec	—	—
DC Square Pulse	45 sec	—	—
RF Modulated Gaussian Pulse	145 sec	5 sec	5 sec
RF Modulated Square Pulse	180 sec	10 sec	5 sec
Simple Arbitrary Pulse	90 sec	—	—
Complex Arbitrary Pulse	180 sec	—	—
Stepped DC Pulse	30 sec	—	—

ond derivatives become

$$\beta(\omega) = \frac{\omega}{c}\sqrt{\epsilon_{r_{\text{eff}}}(\omega)} = \frac{\omega}{c}A \tag{23}$$

$$\beta'(\omega) = \frac{\omega}{c}\frac{B}{A} + \frac{A}{c} \tag{24}$$

$$\beta''(\omega) = 2\frac{B}{cA} - \frac{\omega}{c}\frac{B^2}{A^3} + \frac{\omega}{c}\frac{D}{A} \tag{25}$$

where

$$B = \frac{\omega\left(\epsilon_r - \epsilon_{r_{\text{eff}}}(0)\right)\omega_T^2}{\left(\omega_T^2 + \omega^2\right)^2} \tag{26a}$$

$$D = \frac{B}{\omega} - 4.0B\frac{\omega}{\omega_T^2 + \omega^2} \tag{26b}$$

ϵ_r dielectric constant of substrate,
$\epsilon_{r_{\text{eff}}}(0)$ effective dielectric constant at zero frequency [19].

Figs. 11 and 12 show the envelopes of dispersed RF Gaussian and square pulses computed using the Taylor series expansion method. These are superimposed on RF pulses which have been computed using numerical integration for comparison.

These figures, which show at most approximately 10-percent difference in the amplitudes of the two methods, exhibit pulses with a low repetition rate in comparison to the pulsewidth. The higher the carrier frequency, the better the accuracy of the quadratic approximation.

The computation time for calculating the dispersed waveforms of RF pulses was greatly reduced by using the Taylor series expansion method. Table I gives typical times required to compute dispersed waveforms of various dc and RF pulses using an IBM 3081. It is evident from these and other computations not included here that the Taylor series expansion method yields good waveform approximations to the distorted RF pulses with a considerable reduction in computation time.

VI. CONCLUSIONS

The distortion of dc and RF pulses as they propagate along a microstrip line was investigated using dispersion models in conjunction with numerical integration and Taylor series expansion approximation techniques. Pramanick and Bhartia's dispersion model provided a convenient closed-form equation to evaluate the distortion of a pulse propagating along a microstrip line. Numerical integration was required for dc pulses. Arbitrarily shaped pulses which did not have a closed-form solution for their Fourier transform were evaluated using the segmenting method. RF pulses can be analyzed using either numerical integration or the Taylor series expansion method, with only a slight decrease in accuracy but considerable improvement in computational efficiency.

ACKNOWLEDGMENT

The authors would like to thank Dr. J. W. Mink of the Electronics Division, Army Research Office, for his interest and support of the project, T. Leung for the preparation of the final figures, and T. Griesser for the expert typing of the manuscript.

REFERENCES

[1] M. P. Forrer, "Analysis of millimicrosecond RF pulse transmission," *Proceeding IRE*, vol. 46, pp. 1830–1835, Nov. 1958.
[2] R. S. Elliott, "Pulse waveform degradation due to dispersion in waveguide," *IRE Trans. Microwave Theory Tech.*, vol. MTT-5, no. 10, pp. 254–257. Oct. 1957.
[3] C. M. Knop, "Pulsed electromagnetic wave propagation in dispersive media," *IEEE Trans. Antennas Propagat.*, vol. AP-12, pp. 494–496, July 1964.
[4] K. K. Li *et al.*, "Propagation of picosecond pulses in microwave striplines," *IEEE Trans. Microwave Theory Tech.*, vol. MTT-30, pp. 1270–1272, Aug. 1982.
[5] D. C. Champeney, *Fourier Transforms and their Physical Applications*. New York: Academic Press, 1973, ch. 2, pp. 8–20.
[6] T. Itoh, and R. Mittra, "Spectral-domain approach for calculating the dispersion characteristics of microstrip lines," *IEEE Trans. Microwave Theory Tech.*, vol. MTT-21, pp. 496–499, July 1973.
[7] É. J. Denlinger *et al.*, "A frequency dependent solution for microstrip transmission lines," *IEEE Trans. Microwave Theory Tech.*, vol. MTT-19, pp. 30–39, Jan. 1971.
[8] E. F. Kuester and D. C. Chang, "An appraisal of methods for computation of the dispersion characteristics of open microstrip," *IEEE Trans. Microwave Theory Tech.*, vol. MTT-27, pp. 691–694, July, 1979.
[9] W. J. Chudobiak, O. P. Jain, and V. Makios, "Dispersion in microstrip," *IEEE Trans. Microwave Theory Tech.*, vol. MTT-19, pp. 783–784, Sept. 1971.
[10] C. P. Hartwig, D. Masse, and R. A. Pucel, "Frequency dependent behavior of microstrip," in *Int. Microwave Symp.*, (Detroit, MI), May 1968, pp. 110–116.
[11] W. J. Getsinger, "Microstrip dispersion model," *IEEE Trans. Microwave Theory Tech.*, vol. MTT-21, pp. 34–39, Jan. 1973.
[12] M. V. Schneider, "Microstrip dispersion," *IEEE Trans. Microwave Theory Tech.*, vol. MTT-20, pp. 144–146, Jan. 1972.
[13] H. J. Carlin, "A simplified circuit model for microstrip," *IEEE Trans. Microwave Theory Tech.*, vol. MTT-21, pp. 589–591, Sept. 1973.
[14] M. Kobayashi, "Important role of inflection frequency in the dispersive properties of microstrip lines," *IEEE Trans. Microwave Theory Tech.*, vol. MTT-30, pp. 2057–2059, Nov. 1982.
[15] P. Pramanick and P. Bhartia, "An accurate discription of dispersion in microstrip," *Microwave J.*, pp. 89–96, Dec. 1983.
[16] E. Yamashita, K. Atsuki, and T. Veda, "An approximate dispersion formula of microstrip lines for computer-aided design of microwave integrated circuits," *IEEE Trans. Microwave Theory Tech.*, vol. MTT-27, pp. 1036–1038, Dec. 1979.

[17] M. Kirching and R. H. Jansen, "Accurate model for effective dielectric constant of microstrip with validity up to millimetre-wave frequencies," *Electron. Lett.*, vol. 18, pp. 272–273, 1982.
[18] A. Papoulis, *The Fourier Integral and its Applications*. New York: McGraw-Hill, 1962, ch. 7, pp. 120–143.
[19] I. J. Bahl and D. K. Trivedi, "A designer's guide to microstrip line," *Microwaves*, pp. 174–182, May 1977.

✠

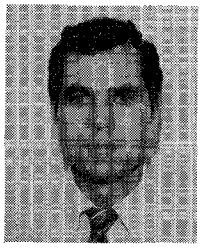

Richard L. Veghte (M'79) was born on November 20, 1956, in Lebanon, MO. He received the B.S. degree in electrical engineering from the University of Colorado in 1979. He has also received the Masters in Business Administration in 1984 and the M.S. in electrical engineering in 1986, both from Arizona State University.

From 1979 to 1982, he worked at Goodyear Aerospace in Phoenix, AZ, as a Design Engineer in the Microwave and Antenna Research and Development group. Since 1983, he has been a member of Technical Staff at Ball Aerospace in Boulder, CO, where he works on various phased-array and communications antennas for their Antenna Division.

Mr. Veghte is a member of Tau Beta Pi and Eta Kappa Nu.

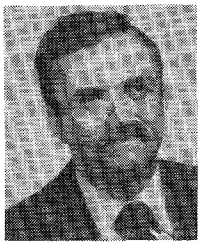

Constantine A. Balanis (S'62–M'68–SM'74–F'86) was born in October, 1938 in Trikala, Greece. He received the B.S.E.E. degree from Virginia Polytechnic Institute, Blacksburg, in 1964, the M.E.E. degree from the University of Virginia, Charlottesville, in 1966, and the Ph.D. degree in electrical engineering from Ohio State University, Columbus, in 1969.

From 1964 to 1970, he was with NASA, Langley Research Center, Hampton, VA. During the period 1968–1970, he also held a part-time appointment as Assistant Professorial Lecturer in the Department of Electrical Engineering, George Washington University, Washington, DC, graduate extension at Langley. In 1970, he joined the Department of Electrical Engineering, West Virginia University, Morgantown, as a Visiting Associate Professor and held the positions of Associate and Full Professor. Since 1983, he has been a Full Professor in the Department of Electrical and Computer Engineering, Arizona State University, Tempe. He teaches graduate and undergraduate courses in electromagnetic theory, microwave circuits, and antennas. His research interests are in low- and high-frequency numerical antenna and scattering techniques, reconstruction (inversion) methods, and electromagnetic wave propagation in microwave-integrated circuit transmission lines.

Dr. Balanis is a member of ASEE, Sigma Xi, Tau Beta Pi, Eta Kappa Nu, and Phi Kappa Phi. He is listed in *American Men of Science*, *Who's Who in the East*, *Who's Who in the South and Southwest*, *Who's Who in Engineering*, *Dictionary of International Biography* (British), *Men of Achievement* (British), and *Who's Who 1979* (Greek). He has served as Associate Editor of the IEEE TRANSACTIONS ON ANTENNAS AND PROPAGATION (1974–1977) and IEEE TRANSACTIONS ON GEOSCIENCE AND REMOTE-SENSING (1982–1984), Editor of the NEWSLETTER for the IEEE Geoscience and Remote Sensing Society 91982–1983), and as Second Vice-President of the IEEE Geoscience and Remote Sensing Society. He has held the positions of Delegate-at-Large, Secretary–Treasurer, Vice-Chairman, and Chairman of the Upper Monongahela IEEE Subsection of the Pittsburgh Section. He is author of *Antenna Theory: Analysis and Design* (New York: Harper and Row, 1982).